Full Paper

Journal of Nano Materials Impact 2025, 01 (01) 19-24

Nonlinear Optical Properties of Core@Shell Nanoparticles of Gold and Moringa Oleifera Leaves via Laser Ablation Technique

Ahmed M. Hassan, Asmahan A. Muhmood*

Department of Physics, Faculty of Science, University of Kufa, Najaf, IRAQ

Abstract

In this paper, gold and Moringa oleifera leaf nanoparticles were synthesized using laser ablation techniques by Nd-YAG laser with a wavelength of 1064 nm, energy of 100 mJ, and a frequency of 3 Hz. The gold plate and Moringa oleifera leaf tablets (after grinding it then being compressed and exposed to heat) were immersed in 5 ml of distilled water for each one individually to synthesize nanoparticles as a first step. The second step was a synthesis of core@shell from gold and Moringa nanoparticles with different pulse numbers (250,500, and 750) pulse where gold was used as the core and Moringa as the shell and vice versa. The prepared samples were characterized using transmission electron microscopy (TEM) and scanning electron microscopy (SEM). The Z-Scan technique with a closed aperture system was used to study the nonlinear optical properties of the prepared samples. The results show the success of the techniques used where the particle size was between (15–50) nm. The nonlinear properties of the prepared samples showed that they have a negative nonlinear refractive index, that is, the nonlinear transmittance curve begins with a peak and is followed by a trough.

Keyword: gold nanoparticles • moringa oleifera nanoparticles • core@shell nanoparticles • laser ablation in liquid.

Introduction

The study of nonlinear optics investigates the nonlinear reactions that occur when intense light interacts with matter. The utilization of nanoparticles created via laser ablation has been widely employed in the realm of nonlinear optics. A nonlinear optical effect refers to a process in which the optical characteristics of a material undergo nonlinear changes due to the powerful irradiation of incident light [1]. Nanoparticles exhibit great potential due to their flexibility to be engineered and their enhanced nonlinear optical properties superior to their bulk counterparts [2].

The production of nanoparticles through laser ablation serves as an environmentally friendly, efficient, and universally applicable physical method that allows for rapid one-step synthesis and potential large-scale manufacturing[3]. Nanostructures can be categorized according to the use of one or multiple materials, resulting in the formation of either basic or composite nanoparticles.

Basic nanostructures are constructed from a singular material, whereas composite nanostructures consist of two or more materials, such as core-shell nanoparticles[4, 5].

***Address for correspondence:** Asst. Prof. Dr. Asmahan A. Muhmood, Department of Physics, Faculty of Science, University of Kufa, Najaf, Iraq.

E-mail: asmahan.alnaseefi@uokufa.edu.iq

ORCID: https://orcid.org/my-orcid?orcid=0000-0002-1989-787X

Info:

Submitted: 01 Nov. 2024; **Revised:** 02 Jan. 2025;

Accepted: 27 Jan. 2025; **Published:** 10 Feb. 2025.

https://doi.org/10.71109/nmi.2025.1.1.7

The nanoparticles of the core-shell type are characterized as having a central core consisting of an inner material and an outer shell composed of a coating material. As it can be seen in **Figure 1**, core@shell nanoparticles can be classified according to the composition of their inner and outer materials, which can be organic-organic, inorganic-inorganic, organic-inorganic, or inorganic-organic [6]. Depending on the specific usage, the selection of shell material, as well as the form and/or composition of nanoparticles, can be determined[7].

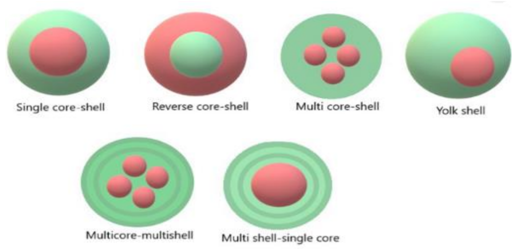

Figure 1. Classification of core@shell nanostructures can be done by considering the number of core and shell components present in the structure [8].

Gold nanoparticles (AuNPs) have been the subject of extensive research in various fields, ranging from materials science to medical science [9, 10] because of their high quality[11], attributes such as being non-toxic and being easily available while possessing controlled size and shape [12, 13], the particle's reactivity at a greater level, the capacity for modifying its surface, as well as its remarkable optical qualities [14].

The Moringa oleifera plant has been widely used in the treatment and management of conditions such as malnutrition and diabetes, in addition to heart and liver diseases [15], and as anti-hypertensive agents [16].

Modified characteristics of core@shell nanoparticles can be achieved through either adjusting the volume ratio between the core and shell components or by altering the composite materials [17]. The primary objective of the core part coating is to manipulate the surface alterations, stability, and dispersibility in order to regulate the functionality of the core [18].

The process wherein material is extracted from the surface of a solid target, which is situated in a vacuum or in a gaseous or liquid environment, through the exposure to laser radiation is referred to as laser ablation. The interaction between laser radiation and matter is contingent upon factors such as the wavelength of the laser [19] , the duration of the pulse [20] , and the intensity of the laser pulse, as well as the thermophysical and optical characteristics of both the target and its surrounding environment. The creation and development of nanoparticles involves various physical processes, including the generation of a plasma plume, condensation, agglomeration, and nucleation [21].

The methodology of pulsed laser ablation in liquid (PLAL) is regarded as a highly favorable top-down approach for the production of nanoparticles that are pure and uncontaminated. This process is relatively rapid, exhibits efficient mass production, and low cost [22]. The arrangement of the LAL setup is comparatively straightforward and expedient, as shown in **Figure 2**.

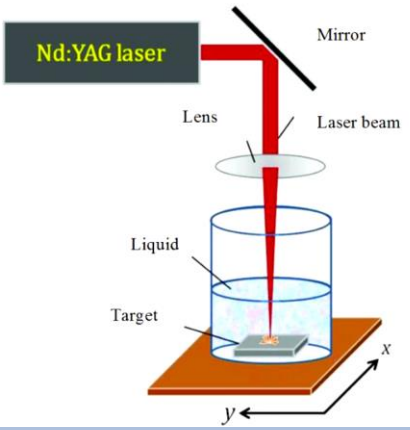

Figure 2. Schematic describing laser ablation in liquid to form core-shell Nanoparticle [23].

Theoretical Background

The maximum transmittance (peak) followed by the minimum transmittance (bottom) is evidence of a negative nonlinear transmittance (negative refractive index). While the Z-scan curve (i.e., a bottom followed by a peak) characterizes the nonlinear transmittance (the material has a positive nonlinear refractive index). **Figure 3** shows the nonlinear transmittance represented by the positive and negative nonlinear refractive index value [24].

The nonlinear refractive index from the peak-to-bottom difference for normal transmittance is calculated (experimentally) by the following formula [25]:

$$n_2 = \frac{\Delta\emptyset_o}{(I_o L_{eff} K)} \quad \dots (1)$$

where: $\Delta\emptyset_o$: The nonlinear phase shift of the peak on the axis at the focus. I_o: Incident light intensity. K : Wave vector, $K = 2\pi/\lambda$ where λ is the wavelength of the beam. L_{eff}:

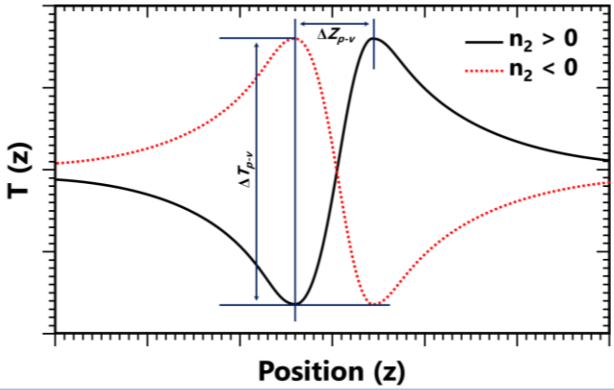

Figure 3. Z-scan technique for positive (black line) and negative (red line) nonlinear refraction.

The effective length of the sample can be determined from the following relationship [26]:

$$L_{eff} = \frac{(1 - e^{-\alpha_o L})}{\alpha_o} \quad \dots (2)$$

Where L: is the length of the model.

Moreover, ΔT_{P-V} is the change in natural transmittance between the top and the bottom and is equal |TP -TV| [27].

$$\Delta T_{P-V} = 0.406(1 - S)^{0.25}|\Delta\phi_o| \quad \dots (3)$$

Where S is equal [26]:

$$S = 1 - \exp\left(\frac{-2r_a^2}{\omega_a^2}\right) \quad \dots (4)$$

Where, S is the linear transmittance of the aperture, r_a is the radius of the aperture, and ω_a is the radius of the laser beam at the aperture.

To calculate the intensity at the focal point (I_o), we use the following equation [25]:

$$I_o = \frac{2P_{peak}}{\pi\omega_a^2} \quad \dots (5)$$

Where ω_0 is the radius of the laser beam at the focus, and P_{peak} is the laser power.

Experimental

A glass jar containing five milliliters of distilled water and a tablet of Moringa oleifera was inside. The sample was then exposed to 500 pulses of a 1064 nm Nd-YAG laser. Keep in mind that this is the first study to use the laser ablation approach to generate Moringa oleifera nanoparticles.

Preparation of Moringa Oleifera Leaf Extract

To create plant leaf tablets with a diameter of 2.5 cm and a thickness of 0.5 cm, the dried leaves of the Moringa oleifera plant were brought, cleaned of impurities, ground, and compressed using a press device at a pressure of 20 MPa. The tablets were then microwave-heated to a temperature of 90° C for three hours to improve their consistency as shown in the **Figure 4**.

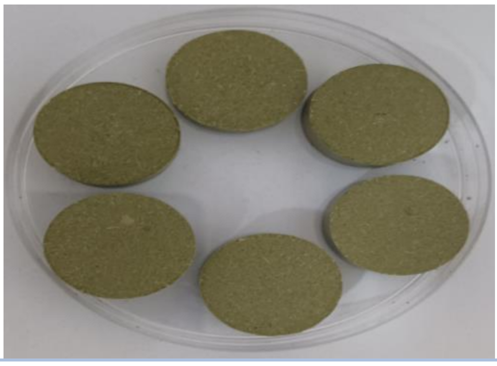

Figure 4. Moringa oleifera leaf tablets.

Synthesis of AuNPs by Laser Ablation

Laser ablation was used to create AuNPs. The ablation procedure was carried out using a Nd-YAG laser with a wavelength of 1064 nm, an energy of 100 mJ, and a frequency of 3 Hz. 500 pulses were applied to a pure gold plate after it had been submerged in 5 milliliters of distilled water to create AuNPs.

Synthesis of Moringa Oleifera Nanoparticles by Laser Ablation

A glass jar containing 5 mL of distilled water and a tablet of Moringa oleifera was inside. The sample was then exposed to 500 pulses of a 1064 nm Nd-YAG laser. Keep in mind that this is the first study to use the laser ablation approach to generate Moringa oleifera nanoparticles.

Synthesis of Au@Mo NPs by Laser Ablation

To prepare Au@Mo core@shell nanoparticles using laser ablation technique in liquids. AuNPs were prepared by bombarding a gold plate in 5 mL of distilled water with 750 pulses of an Nd-YAG laser. The gold plate was then replaced with a Moringa leaf disc in the liquid containing AuNPs and the sample was bombarded with 500 pulses. Then we repeated the process by bombarding the gold plate with 500 pulses of laser in distilled water and replacing it with a Moringa plant disc and bombarding it with 250 pulses as shown in **Table 1**.

Table 1. The number of pulses used in preparation of Au@Mo NPs.

core@shell NPs	Au	Mo
Au@Mo	750 pulses	500 pulses
Au@Mo	500 pulses	250 pulses

Synthesis of Mo@Au NPs by Laser Ablation

An Nd-YAG laser was utilized for bombarding a Moringa plant disc in 5 milliliters of distilled water with 750 pulses in order to create Moringa nanoparticles. After that, the plant sample was replaced out with a gold plate submerged in a solution containing Moringa nanoparticles, and 500 pulses were applied. Then we repeated the process, but this time by bombarding the Moringa plant disc with 500 laser pulses in distilled water, replacing it with a gold plate, and bombarding it with 250 pulses as shown in **Table 2**.

Table 2. The number of pulses used in preparation of Mo@Au NPs.

core@shell NPs	Au	Mo
Mo@Au	750 pulses	500 pulses
Mo@Au	500 pulses	250 pulses

Results and Discussion

The synthesis of Au, Mo as Au@Mo and Mo@Au core-shell NPs were performed via laser ablation in distilled water. After seconds of ablation, the color of solutions changes, as shown **Figure 5** which show an image for gold and Moringa oleifera NPs individually, Au@Mo NPs, and Mo@Au NPs.

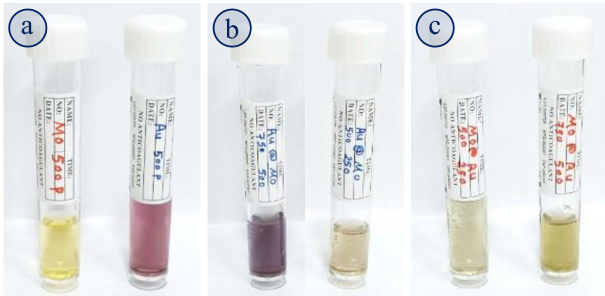

Figure 5. Photograph of (a) Au and Mo NPs, (b) Au@Mo NPs and (c) Mo@Au NPs.

The Z-Scan technique with a closed aperture system was used to calculate the nonlinear refractive index of the prepared samples. We notice in **Figures 6a-6d** display the nonlinear transmittance of Au, Mo, Au@Mo, and Mo@Au NPs under the influence of a wavelength (532 nm) and a power of 25.24 mW using a confocal lens with a focal length of 8.5 cm. We note that the samples have a nonlinear refractive index of a negative value, that is, the nonlinear transmittance curve begins with a peak and is followed by a trough.

We note that the difference between the peak and bottom of the nonlinear transmittance curve increases with the increase in the number of laser pulses used (increasing the concentration of nanoparticles), as in the Figures 6c and 6d, meaning that the effect of increasing the concentration clearly affects the nonlinearity of the material. **Table 3**. shows the nonlinear properties of the samples. We note the increase in the absolute value of the nonlinear refractive index due to the increase in concentration.

To ensure the formation of nanoparticles of Au@Mo, and Mo@Au, the prepared samples were examined using the field emission scanning electron microscopy (FESEM) and the transmission electron microscopy (TEM). **Figure 7a** shows the surface morphology of the Au@Mo NPs using the FESEM. Moreover, the respective particle size histogram displays in Figure 7b, the estimated average particle size was 22.13 nm.

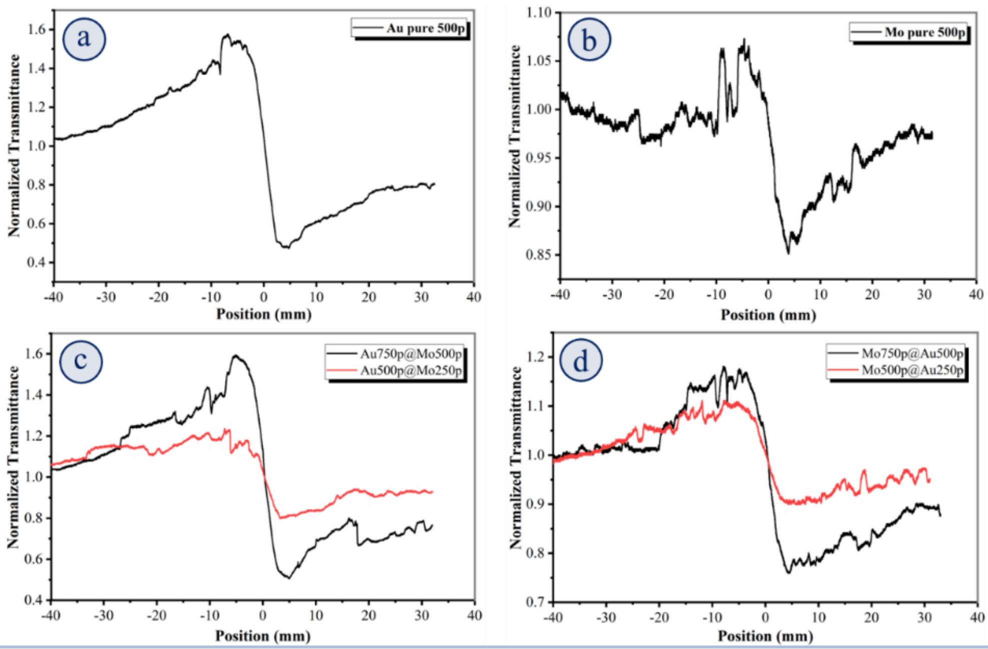

Figure 6. Nonlinear refraction of (a) Au NPs, (b) Mo NPs, (c) Au@Mo NPs, and Mo@Au NPs.

Table 3. Nonlinear properties of prepared samples.

Concentration	P (mW)	λ (nm)	f (cm)	I_o (MW/m^2)	L_{eff} (m)	ΔT	S	n2 (m^2/W)
Au NPs	25.24	532	8.5	13.2909	0.000974	1.106195	0.076884	-1.82E-11
Mo NPs	25.24	532	8.5	13.2909	0.000996	0.222222	0.076884	-3.57E-12
Au750p@Mo500p NPs	25.24	532	8.5	13.2909	0.000972	1.089888	0.076884	-1.80E-11
Au500p@Mo250p NPs	25.24	532	8.5	13.2909	0.00099	0.439474	0.076884	-7.11E-12
Mo750p@Au500p NPs	25.24	532	8.5	13.2909	0.000985	0.42228	0.076884	-6.86E-12
Mo500p@Au250p NPs	25.24	532	8.5	13.2909	0.000992	0.212202	0.076884	-3.43E-12

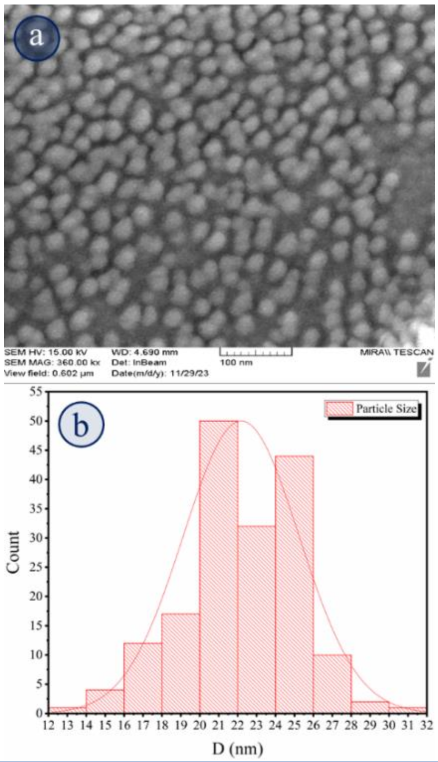

Figure 7. (a) FESEM micrograph of Au@Mo NPs, (b) the respective particle size histogram.

Figure 8a shows the surface morphology of the (Mo@Au) NPs and **Figure 8b** the respective particle size histogram, the average particle size was (23.83 nm). Scale bars correspond to a length of 100 nm.

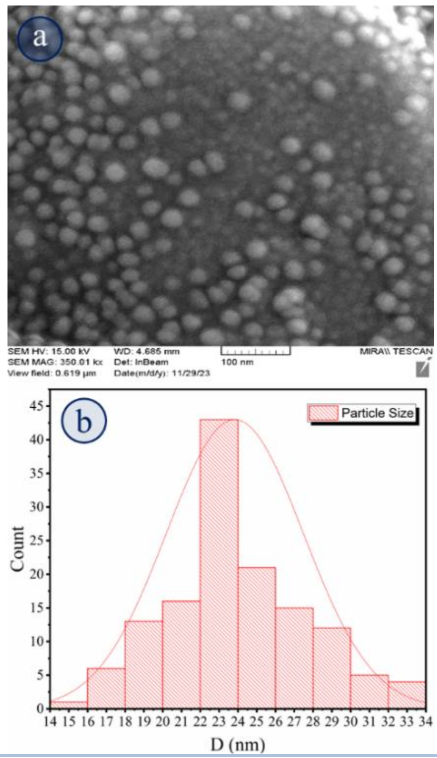

Figure 8. (a) FESEM micrograph of Mo@Au NPs and (b) the respective particle size histogram.

The results of the TEM image show the formation of a core shell nanoparticles model for Au@Mo as in **Figure 9a**, where the number of laser pulses was 750 pulses for gold and 500 pulses for Moringa, and Mo@Au NPs in **Figure 9b** with a number of pulses of 750 pulses for Moringa and 500 pulses for gold, which shows the sphericality of the nanoparticles formed with some particles appearing in irregular shapes.

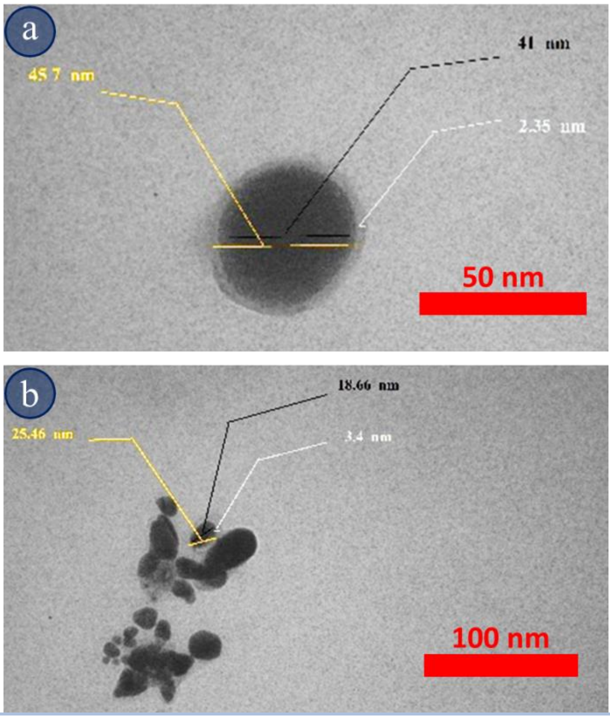

Figure 9. TEM micrograph of (a) Au@Mo and (b) Mo@Au NPs.

Conclusion

The laser ablation method used to prepare core shell nanoparticles is easy, low-cost and Eco-friendly (no toxic materials used). Tests showed the successful formation of a core shell pattern between the gold and the leaves of the Moringa plant, and the sizes of the nanoparticles ranged from 15 to 50 nanometers, depending on the tests used, and they have a negative nonlinear refractive index (the nonlinear transmittance curve begins with a peak followed by a trough), and the difference between the peak and trough in this curve increases. By increasing the concentration of nanoparticles formed in the core shell model in both gold metal and Moringa oleifera leaves.

Acknowledgements

In this work, we would like to extend our thanks to the Department of Laser Physics, Faculty of Science for Women, University of Babylon for their cooperation with our team.

Declaration of Competing Interests

The authors declare that they have no conflicts of interest

References

[1] R. W. Boyd, A. L. Gaeta, and E. Giese, "Nonlinear Optics," in *Springer Handbook of Atomic, Molecular, and Optical Physics*, G. W. F. Drake, Ed. Cham: Springer, 2023, pp. 1097-1110. https://doi.org/10.1007/978-3-030-73893-8_76.

[2] A. K. H. Albarazanchi, A. Al-Haddad, and M. F. Sultan, "Plasmonic Enhancement Mechanism of Template-Based Synthesized Au@TiO_2 Nanodiscs," *ChemNanoMat*, vol. 7, no. 1, p. 27-33, 2021. https://doi.org/10.1002/cnma.202000513.

[3] L. Chen and M. Hong, "Functional nonlinear optical nanoparticles synthesized by laser ablation," *Opto-Electronic Science*, vol. 1, no. 5, p. 210007-1-210007-25, 2022. https://doi.org/10.29026/oes.2022.210007.

[4] P. Mélinon *et al.*, "Engineered inorganic core/shell nanoparticles," *Physics Reports*, vol. 543, no. 3, p. 163-197, 2014. https://doi.org/10.1016/j.physrep.2014.05.003.

[5] W. Lv, P. E. Phelan, R. Swaminathan, T. P. Otanicar, and R. A. Taylor, "Multifunctional core-shell nanoparticle suspensions for efficient absorption," *Journal of solar energy engineering*, vol. 135, no. 2, p. 021004, 2013. https://doi.org/10.1115/1.4007845.

[6] R. Ghosh Chaudhuri and S. Paria, "Core/shell nanoparticles: classes, properties, synthesis mechanisms, characterization, and applications," *Chemical reviews*, vol. 112, no. 4, p. 2373-2433, 2012. https://doi.org/10.1021/cr100449n.

[7] R. Liu and R. D. Priestley, "Rational design and fabrication of core–shell nanoparticles through a one-step/pot strategy," *Journal of Materials Chemistry A*, vol. 4, no. 18, p. 6680-6692, 2016. https://doi.org/10.1039/C5TA09607C.

[8] R. Singh and R. Bhateria, "Core–shell nanostructures: a simplest two-component system with enhanced properties and multiple applications," *Environmental Geochemistry and Health*, vol. 43, p. 2459-2482, 2021. https://doi.org/10.1007/s10653-020-00766-1.

[9] A. M. Gamal-Eldeen *et al.*, "Photothermal therapy mediated by gum Arabic-conjugated gold nanoparticles suppresses liver preneoplastic lesions in mice," *Journal of Photochemistry and Photobiology B: Biology*, vol. 163, p. 47-56, 2016. https://doi.org/10.1016/j.jphotobiol.2016.08.009.

[10] L. Torrisi and A. Torrisi, "Laser ablation parameters influencing gold nanoparticle synthesis in water," *Radiation Effects and Defects in solids*, vol. 173, no. 9-10, p. 729-739, 2018. https://doi.org/10.1080/10420150.2018.1528598.

[11] D. Xi, S. Dong, X. Meng, Q. Lu, L. Meng, and J. Ye, "Gold nanoparticles as computerized tomography (CT) contrast agents," *Rsc Advances*, vol. 2, no. 33, p. 12515-12524, 2012. https://doi.org/10.1039/c2ra21263c.

[12] H. R. de Barros *et al.*, "Stability of gum arabic-gold nanoparticles in physiological simulated pHs and their selective effect on cell lines," *RSC Advances*, vol. 6, no. 12, p. 9411-9420, 2016. https://doi.org/10.1039/C5RA24858B.

[13] O. B. Adewale, H. Davids, L. Cairncross, and S. Roux, "Toxicological behavior of gold nanoparticles on various models: influence of physicochemical properties and

other factors," *International journal of toxicology*, vol. 38, no. 5, p. 357-384, 2019. https://doi.org/10.1177/1091581819863130.

[14] I. Fratoddi *et al.*, "Highly hydrophilic gold nanoparticles as carrier for anticancer copper (I) complexes: Loading and release studies for biomedical applications," *Nanomaterials*, vol. 9, no. 5, p. 772, 2019. https://doi.org/10.3390/nano9050772.

[15] H. M. Hassan *et al.*, "Modulatory effects of Moringa oleifera leaf extract on sodium nitrate-induced experimental colitis via regulation of P53, Ki-67 and PCNA biomarkers," *Tissue and Cell*, vol. 88, p. 102327, 2024. https://doi.org/10.1016/j.tice.2024.102327.

[16] S. Faizi, B. S. Siddiqui, R. Saleem, S. Siddiqui, and K. Aftab, "Fully acetylated carbamate and hypotensive thiocarbamate glycosides from Moringa oleifera," *Phytochemistry*, vol. 38, no. 4, p. 957-963, 1995. https://doi.org/10.1016/0031-9422(94)00729-D.

[17] E. Hamidi-Asl, F. Dardenne, S. Pilehvar, R. Blust, and K. De Wael, "Unique properties of core shell Ag@ Au nanoparticles for the aptasensing of bacterial cells," *Chemosensors*, vol. 4, no. 3, p. 16, 2016. https://doi.org/10.3390/chemosensors4030016.

[18] G. Baffou, R. Quidant, and C. Girard, "Heat generation in plasmonic nanostructures: Influence of morphology," *Applied Physics Letters*, vol. 94, no. 15, 2009. https://doi.org/10.1063/1.3116645.

[19] A. Hussein, P. Diwakar, S. Harilal, and A. Hassanein, "The role of laser wavelength on plasma generation and expansion of ablation plumes in air," *journal of applied physics*, vol. 113, no. 14, 2013. https://doi.org/10.1063/1.4800925.

[20] B. Verhoff, S. Harilal, J. Freeman, P. Diwakar, and A. Hassanein, "Dynamics of femto-and nanosecond laser ablation plumes investigated using optical emission spectroscopy," *Journal of Applied Physics*, vol. 112, no. 9, 2012. https://doi.org/10.1063/1.4764060.

[21] S. Bashir, M. S. Rafique, C. S. Nathala, and W. Husinsky, "Surface and structural modifications of titanium induced by various pulse energies of a femtosecond laser in liquid and dry environment," *Applied Physics A*, vol. 114, p. 243-251, 2014. https://doi.org/10.1007/s00339-013-8116-2.

[22] E. Fazio *et al.*, "Nanoparticles engineering by pulsed laser ablation in liquids: Concepts and applications," *Nanomaterials*, vol. 10, no. 11, p. 2317, 2020. https://doi.org/10.3390/nano10112317.

[23] Y. Herbani, R. Nasution, F. Mujtahid, and S. Masse, "Pulse laser ablation of Au, Ag, and Cu metal targets in liquid for nanoparticle production," in *Journal of Physics: Conference Series*, 2018, vol. 985, no. 1, p. 012005: IOP Publishing. https://doi.org/10.1088/1742-6596/985/1/012005.

[24] S. Gomez, F. Cuppo, and A. M. Figueiredo Neto, "Nonlinear optical properties of liquid crystals probed by Z-scan technique," *Brazilian Journal of Physics*, vol. 33, p. 813-820, 2003. https://doi.org/10.1590/S0103-97332003000400035.

[25] A. Dhinaa and P. Palanisamy, "Z-Scan technique: To measure the total protein and albumin in blood," *J. Biomed. Sci. Eng*, vol. 3, no. 03, p. 285-290, 2010. https://doi.org/10.4236/jbise.2010.33038.

[26] P. Chapple, J. Staromlynska, J. Hermann, T. Mckay, and R. McDuff, "Single-beam Z-scan: measurement techniques and analysis," *Journal of Nonlinear Optical Physics & Materials*, vol. 6, no. 03, p. 251-293, 1997. https://doi.org/10.1142/S0218863597000204.

[27] A. A. Ali, V. Sindhu, and A. Srinivasan, "Third order nonlinear optical studies of bromocresol purple in liquid and solid media," *Optik*, vol. 124, no. 21, p. 4836-4840, 2013. https://doi.org/10.1016/j.ijleo.2013.02.032.